

# Concept and cable-tensioning optimization of post-tensioned shells made of structural glass

Francesco LACCONE\*, Luigi MALOMO<sup>a</sup>, Maurizio FROLI<sup>b</sup>, Paolo CIGNONI<sup>a</sup>,  
Nico PIETRONI<sup>c,a</sup>

\* ISTI - CNR and DESTEC - University of Pisa  
via Giuseppe Moruzzi 1, 56124 Pisa, Italy  
francesco.lacone@isti.cnr.it; francesco.lacone@destec.unipi.it

<sup>a</sup> ISTI - CNR

<sup>b</sup> DESTEC - University of Pisa

<sup>c</sup> University of Technology Sydney

## Abstract

Shells made of structural glass are charming objects from both the aesthetics and the engineering point of view. However, they pose two significant challenges: the first one is to assure adequate safety and redundancy concerning possible global collapse; the second one is to guarantee the economy for replacing collapsed components. To address both requirements, this research explores a novel concept where triangular panels of structural glass are both post-tensioned and reinforced to create 3D free-form systems. Hence, the filigree steel truss, made of edges reinforcements, is sized in performance-based perspective to bear at least the weight of all panels in the occurrence of simultaneous cracks (worst-case scenario). The panels are post-tensioned using a set of edge-aligned cables that add beneficial compressive stress on the surface. The cable placement and pre-loads are optimized to minimize the tensile stress acting on the shell and match the manufacturing constraints. These shells optimize material usage by providing not only a transparent and fascinating building separation but also load-bearing capabilities. Visual and structural lightness are improved to grid shell competitors.

**Keywords:** conceptual design, glass structures, thin shell, fail-safe, reinforcement, post-tensioning, cables, optimization.

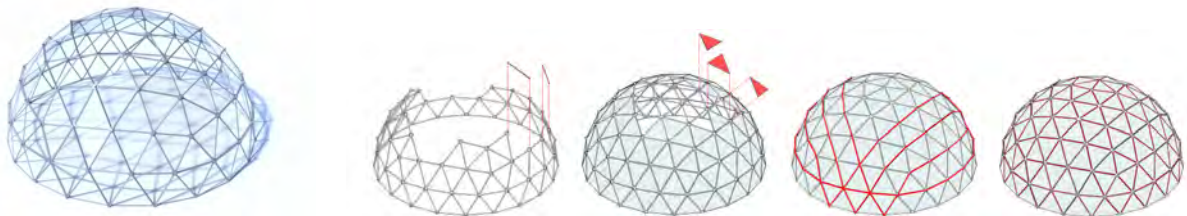


Figure 1: Semi-sphere case study: impression and assembly procedure (skeleton assembly; panels lying; post-tensioning; edge sealant).

## 1 Introduction

Glass is nowadays the most common employed building material for structures, façades, and envelopes that requires a high degree of transparency. Usually, transparent shells are realized as grid shells, in which the grid bearing steel structure is optimized to support large and complex shapes, and the glass is used as cladding [1]. Nevertheless, a recent trend is to maximize the immaterial appearance of the structure and to leave the load bearing function to glass [2]. For shells, a few exemplars are representing a niche category that uses glass as a primary load-bearing material.

Glass-steel systems can be divided into two main categories, depending on their static behavior:

1. Strut-and-tie or tensegrity behavior is founded on a nodal force transfer that activates strut zones along glass panels edges, while the steel profiles - if present - act as ties. In return, the nodes are high-stressed zones and need special design and assembly care. The adopted panels are usually triangular or braced quads. The static response of these structures is akin to grid shells. Examples of these structures are the post-tensioned dome at *Weltbild Verlag* building in Augsburg [3] and the *Maximilianmuseum* roof [4].
2. Shell behaviour is akin to continuous shells, i.e the surface offers a continuous global resistance. The linear joining system enables an uninterrupted transfer of loads between the panel edges. Consequently, it reduces stress concentrations and increases the efficiency of the glass panels. In this case, polygonal panels (usually quads or hexagons) might be preferred to triangles as they offer major redundancy, due to a larger number of edges. Examples of these structures are the Delft dome [5], Blandini's dome [6] and Plate shell structures [7],

Strut-and-tie structures are more diffuse, hence they have been extensively tested, including for failure scenarios such as the complete collapse of panels. On the other hand, shell structures possess more local redundancy: if a single panel is weakened by a crack, the membrane behavior distributes the load on alternative paths. However, the complete collapse of single or multiple panels appears not managed.

Generally, glass structures adopt additional safety layers to avoid dangerous brittle failures. Apart from tempering and lamination, these additional support can be provided by mechanical collaboration with other materials.

Glass and steel collaboration is particularly fruitful and is used to realize mono-dimensional elements (such as beams and columns) or simple bi-dimensional elements (arches, domes, barrel vaults, shear walls). Similarly to rebars in Reinforced Concrete (RC) structures, reinforced glass elements [8] use steel as a ductile material to carry tensile loads. Steel reinforcement sustains the shards of glass from falling and offers redundancy in case the cracking of glass. At the same time, it increases the overall ductility of the structure.

An additional improvement might be provided if steel (bars, cables, strands etc.), as in post-tensioned concrete, is used to install a pre-compression regime on the glass [9].

The present work pursues the Strut-and-tie approach and develops the research of Froli [10, 11] on TVT post-tensioned glass beams. The objective is to realize shells using glass as primary bearing material expanding the possibilities for larger spans or free form geometries, and achieving aesthetic quality (more transparency) and structural efficiency.

The structural concept for these shells is linked to a more general framework that also includes dual layer structures [12]. Optimized in-plane cables are employed to compress glass, conferring it an apparent traction resistance. Conversely, Todisco *et al.* [13] optimize external cables post-

tensioning but in out-of-plane configuration to achieve funicularity in non-funicular structures via Graphic Statics.

The design of these structures [14] is automatically derived through a bespoke statics-aware algorithm which is able to manage, among other constraints, the optimal post-tensioning load provided by a set of edge-aligned cables [15]. The concept and the algorithm are presented in the next section. Several examples are analysed and discussed to validate this approach and to provide quantitative information.

## 2 Reinforced and post-tensioned glass shells

### 2.1 Conceptual design

This research explores a novel structural concept where glass is both post-tensioned and reinforced (fig. 1). These structures addresses two important requirements. The first one is to assure adequate safety and redundancy concerning possible global collapse adopting a Fail-Safe Design [2]. The second one is to avoid damages, especially on the glass, or at least to guarantee a cheap and easy replacing of collapsed components, following the Damage Avoidance Design (DAD) principles [16]. The glass surface is split into triangular panels with rounded corners, clamped into dry mono-lateral steel nodes equipped with spacers. The nodes are a fundamental component of the system because they also merge the reinforcement bars and post-tensioning cables. Other DAD features, such as energy dissipation and post-event serviceability, were already observed in TVTs experimental tests and are expected in the present shells.

The reinforcement bars are located at all edge of panels (fig. 2). Hence they form a triangulated truss (skeleton) that can be sized to withstand at least the weight of the panels. This expedient enhances the redundancy with respect to the Worst Case Scenario (WCS) in which all panels are considered cracked and so only a dead load.

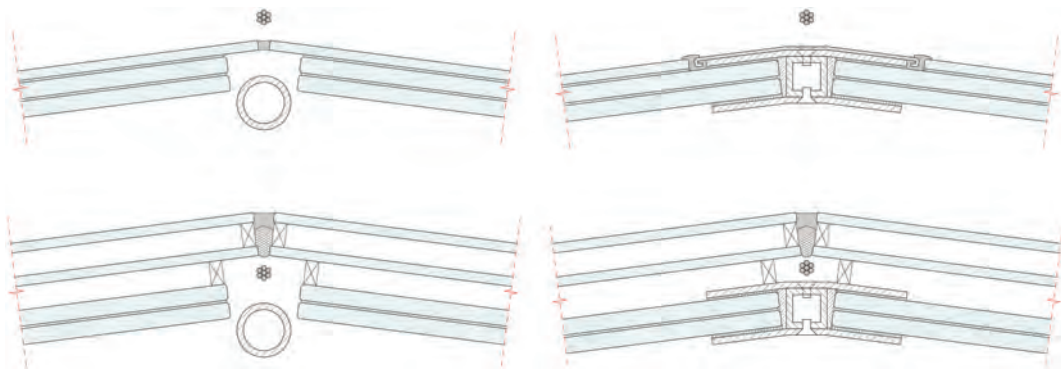


Figure 2: Edge detail with structural laminated glass package, hollow rod as reinforcement (without and with mutual restraint) and spiral cable: (top) with sacrificial glass layer; (bottom) with IGU

### 2.2 Morphogenesis and optimization

Since all triangular edges are reinforced, post-tensioning forces can be exerted by cables along dedicated paths, that is only where the glass must be compressed. The equilibrium of the hybrid structure is guaranteed since the reinforcement can sustain tensile forces, and simultaneously, glass can escape positive stresses because the panel corner can detach from the nodal cap. The skeleton of reinforcements realizes a self-supporting structure, which can be effectively used in

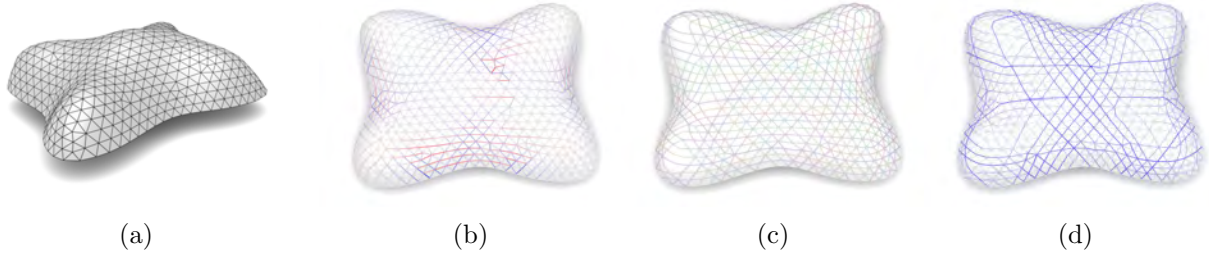


Figure 3: Morphogenesis pipeline: (a) regular remeshing of the input surface; (b) SLS stress on the linear truss model subject to an external load (red compression, blue tension); (c) set of candidate cables; (d) resulting stress on the truss model after the optimization with selected cables and pre-loads.

the assembly phase.

This optimization is formulated as a mixed integer quadratic problem, whose basic assumptions are thin shell theory, linearity and negligible loss of pre-load. Input data of the problem are a membrane or quasi-membrane surfaces and their boundary supports.

The pipeline includes the following steps (refer to fig. 3):

- Surface triangular meshing, to build a quasi-isotropic panel tassellation (fig. 3(a));
- Generation of a linear truss model, where each edge stiffness includes the contribution of both glass and the bar, and computation of stress caused by SLS uniformly distributed load (fig. 3(b));
- Generation of a large set of cables by joining subsequent mesh edges (forming angles not smaller than  $40^\circ$ ) until a border is hit or a loop is formed (fig. 3(c));
- Individual solutions of the truss subject to each cable loading;
- Superimposition of effect and selection of an optimal subset of cables with appropriate pre-loads such that the overall tensile stress is minimized (fig. 3(d)).

Additional constraints are imposed to limit the maximum truss compression and the maximum cable pre-load. This workflow has been implemented in Matlab [17] and C++ environment, in particular using the VCG Library. Several case studies analyzed show an almost complete null of tension stress on the equivalent truss model and an impressive increase of the buckling multiplier with respect to the non-post-tensioned shell.

All case studies use triangular laminated heat-strengthened glass panes ( $8 + 8mm$  with  $1.52mm$  PVB interlayer) and reinforcement bars (hollow steel profile) of  $33.7mm$  outer diameter and  $4mm$  thickness. The target edge of the mesh is  $1m$ . Cables have steel  $15mm$  in diameter.

### 3 Design exploration

Some of the case studies previously optimized in [15] are analyzed by means of global nonlinear analyses in the FEM package Straus7 [18] and discussed. These tests are not meant to be exhaustive of all phenomena, but only to catch the shells global performance. The modeling phase has been supported by the TVT state of the art [19], especially for the calibration of contacts.

For each case, the extracted results are: (i) axial forces and stress field in the post-tensioning phase (in order to check if glass effectively undergoes compression stresses in the assembly); (ii) axial forces and stress field at SLS; (iii) axial forces and stress field at the ULS; (iv) redundancy rate  $R$ . The latter quantity is obtained as the ratio between the safety factors for the ULS load combination of the structure  $SF_{hyb}$  over the safety factor in the WCS  $SF_{WCS}$ . The WCS

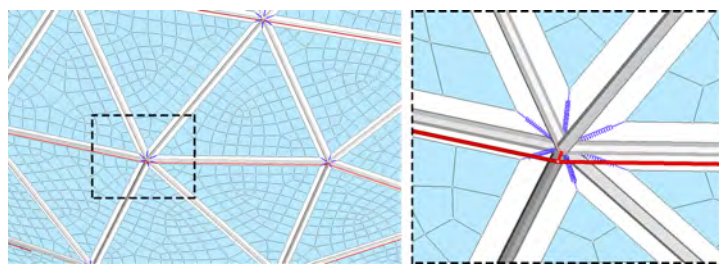


Figure 4: Modelling of the node and merging elements adopted for the FEM analysis

Table 1: Metrics and analysis results on different models (see fig. 5)

Name	Nodes	Panels	Size (m)	Rods	Cables	Buck.mult. $\lambda$	$SF_{hyb}/SF_{WCS} = R$
Vault	506	931	19.1x20.3x6.9	1436	59	14.69	3.12/1.65=1.46
Simplilium	582	1090	25.7x24.2x6.3	1671	48	15.22	5.58/3.14=2.57
Calla	557	1036	20.8x16.0x8.6	1593	56	17.91	3.85/1.54=2.50
Bean	429	796	21.7x16.7x5.7	1224	38	19.12	5.88/3.14=1.87

scenario is simulated in a separate model where the plates are substituted with load patches, non-structural elements for area load distribution.

### 3.1 FE modelling

Nonlinear static analyses are performed to take into account mono-lateral connections (contact non-linearities), shrinkage in the post-tensioning phase and geometric nonlinearities. However, since these analyses already involve a considerable number of variables, material non-linearities have been neglected. Characteristic values are adopted for materials.

The cable pre-load is applied through tension-only elements simultaneously with the dead load. The dead load  $G_1$  is automatically computed from the element property definition, moreover, an additional uniformly-distributed vertical  $Q_k = 1.00kN/m^2$  loading acting on the panels (in the direction of gravity, i.e. snow loading) is superimposed.

Steel reinforcements are modeled as beams, however, both bending and torsion are negligible. Steel nodes where rods merge are dimensionless nodes, with the additional effect of augmenting the slenderness of the rods, ignoring the node encumbrance (fig. 4). The glass-to-steel link is a spring with axial capacity (to resist deformations along its axis), lateral (for all lateral movements) and twist resistance (about its axis). The bending constraint that in real cases, is given by the steel caps is not included. The modeling of panel moreover suggests that peak stresses that may arise in the tip closeness because of force concentration. Stress verification is meaningless in this phase and are demanded to successive detailing design. Monolithic plate elements are used for glass panes and are re-meshed with an eight-node quadrilateral FE (Quad8). The cables are modeled as tension-only segments, which nodes are assumed to be coupled to the frame nodes. In the current analysis border conditions for all models are pin joints and correspond to their boundary vertices.

### 3.2 Results and discussion

The results of nonlinear analyses are shown in tab. 1 and in figs. 5 and 6. The main objective is achieved since all optimized cases manifest low tensile stresses on panels and low positive axial

forces on rods at SLS even in the nonlinear model. Glass pre-compression is diffuse and uniform in the assembly phase, while from the SLS phase, de-compression spreads and high stresses are located in adjacency to post-tensioned edges (principal stress  $\sigma_{22}$  reported in grey scale in fig. 5). In all cases, the safety factors result  $SF_{hyb} \geq 3.00$  and  $SF_{WCS} \geq 1.00$ , with a redundancy always larger than unitary  $R \geq 1.00$ . For an effective comparison of both the design scenario, the full ULS load is considered. The comparison of axial forces can be then considered as a comparison between the present structures and grid shells in terms of steel utilization and stress map. In this regard, the spectrum of axial forces is very reduced with the center of distribution on negative values, while on the WCS side a larger and scattered range of values can be noted.

Grid shells are principal competitors of the shells here investigated. Effective criteria cannot be based on the steel resistance, because it would penalize grid shells. Instead, the two structures can be compared if they both have the same buckling multiplier. So, for each case study the cross-section properties of the grid shell are varied (among those present in commercial catalogs) to match the value of the buckling multiplier  $\lambda$  (ref. tab. 1). Using hollow steel beams in grid shells, both the outer diameter and thickness can be tuned. Usually, for comparable performances, the diameter should be doubled, and the total weight is also roughly doubled. The overall transparency of the structure will be inevitably affected by the new size of the beam. Instead, with solid steel beams, the cross-section is more compact, but however bigger and, even worse, the total weight of the steel will be roughly quintupled.

## 4 Conclusion

Transparent shells can be realized as piecewise assembly of structural glass triangular panels both reinforced with unbonded steel rods and post-tensioned by cables. The specific concept proposed provides safe highly-transparent structures with broad applicability, also in the context of free form architecture.

The structural safety can be deemed appropriate since the panel is mostly compressed at the SLS, and the structure is uniformly and diffusely loaded. A high redundancy with respect to the WCS is stated within the investigated case studies.

These structures might fit the target category of the intermediate-spanned thin-shell structures, in which grid shells are the principal competitors. Making use of structural glass demonstrates advantages in terms of both visual and structural lightness.

## References

- [1] S. Adriaenssens, P. Block, D. Veenendaal, and C. Williams, *Shell structures for architecture: form finding and optimization*, Routledge, 2014.
- [2] M. Haldimann, A. Luble, and M. Overend, *Structural use of glass*, volume 10, Iabse, 2008.
- [3] J. Wurm, *Glass Structures, Design and Construction of Self-supporting Skin*, Birkhäuser, Berlin (Germany), 2007.
- [4] J. J. Ludwig, and H.-U. Weiler, “Tragstrukturen aus Glas am Beispiel einer Ganzglastonnen-Schalenkonstruktion ohne tragende Stahlunterkonstruktion am Maximilianmuseum in Augsburg,” *Bautechnik*, 77(4), pp. 246-249, 2000.
- [5] F. A. Veer, J. Wurm, and G. J. Hobbelman, “The design, construction and validation of a structural glass dome,” *Proceedings of the Glass Processing Days*, Poster, 12, vol. 12, 2003.

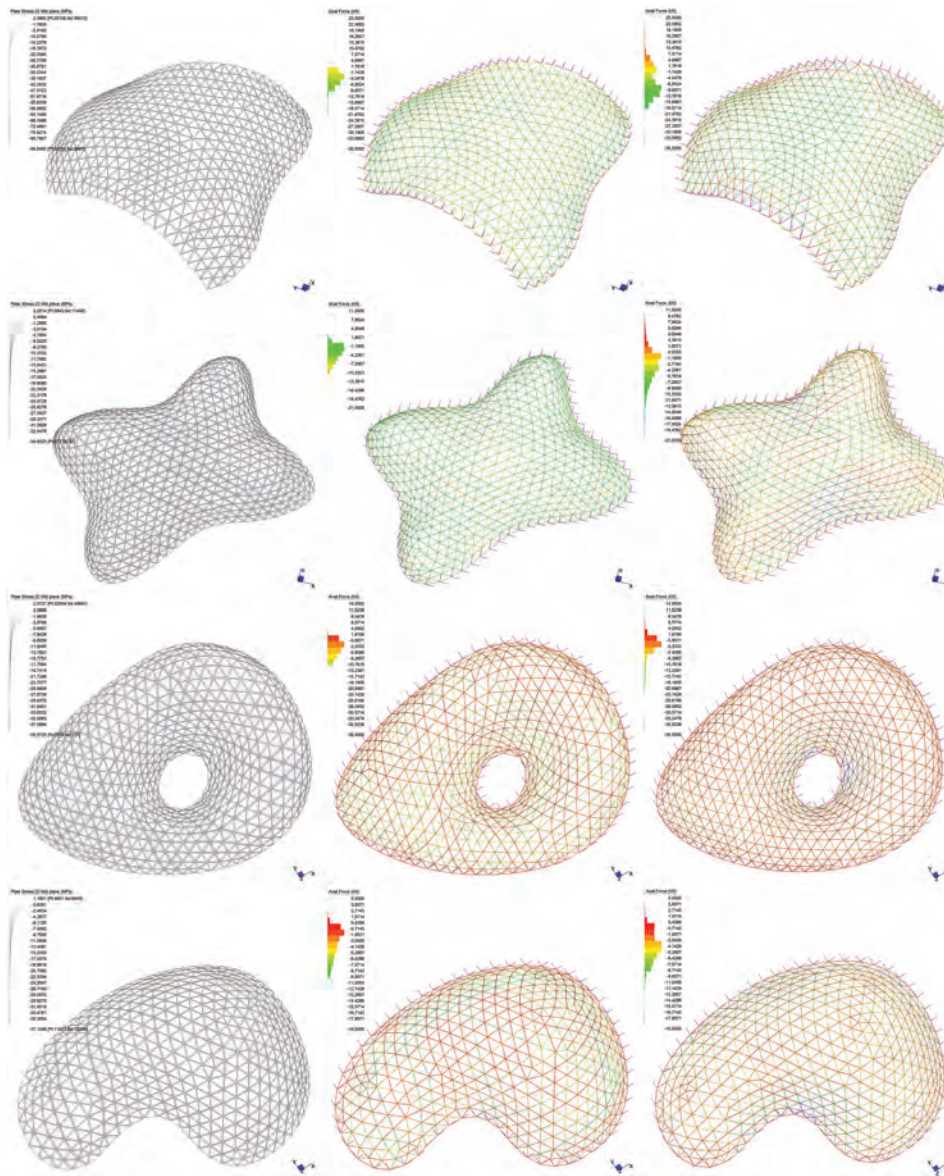


Figure 5: Results of non-linear analyses on Vault, Simplilium, Calla and Bean case studies: (left) glass  $\sigma_{22}$  at SLS; (center) truss axial forces at the ULS; (right) axial forces in the WCS (glass cracked)

- [6] Blandini, L. 2005. *Structural use of adhesives in glass shells*, PhD thesis, Institut für Leichtbau Entwerfen und Konstruieren (ILEK), Universität Stuttgart.
- [7] Bagger, A. 2010. *Plate shell structures of glass: Studies leading to guidelines for structural design* PhD thesis, Technical University of Denmark (DTU).
- [8] K. Martens, R. Caspeele, and J. Belis, “Development of composite glass beams - a review,” *Engineering Structures*, 101, pp. 1-15, 2015.
- [9] K. Martens, R. Caspeele, and J. Belis, “Development of reinforced and posttensioned glass beams: review of experimental research,” *Journal of Structural Engineering*,

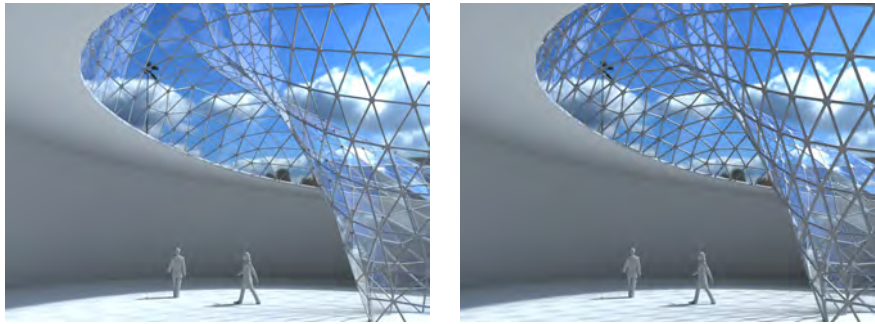


Figure 6: Visual comparison (Calla case study) between the present glass shell (left)) and a classical grid shell with same tessellation and comparable buckling factor (right). Hollow steel beams of 63.5mm outer diameter and 4mm thickness are used for the grid shell (double section size and weight).

142(5):04015173, 2015.

- [10] M. Froli, and L. Lani, “Glass Tensegrity Trusses,” *Structural Engineering International*, 20.4, pp. 436-441, 2010. doi:10.2749/101686610793557564
- [11] M. Froli, and V. Mamone, “A 12 meter long segmented, post-tensioned steel-glass beam (TVT Gamma),” *Challenging Glass 4 & COST Action TU0905 Final Conference*, pp. 243-251, 2014.
- [12] M. Froli, and F. Laccone, “Static concept for long span and high-rise glass structures,” *Journal of Architectural Engineering*, 24.1, 04017030, 2018. doi:10.1061/(ASCE)AE.1943-5568.0000285
- [13] L. Todisco, C. Fivet, H. Corres-Peiretti, and C. Mueller, “Design and exploration of externally post-tensioned structures using graphic statics,” *Journal of the International Association for shell and Spatial Structures*, 56(4), pp.249-258, 2015.
- [14] F. Laccone, *Reinforced and post-tensioned structural glass shells: Concept, morphogenesis and analysis*, PhD thesis, University of Pisa, 2019.
- [15] F. Laccone, L. Malomo, M. Froli, P. Cignoni, N. Pietroni, “Automatic Design of Cable-Tensioned Glass Shells,” *Computer Graphics Forum* 2019. doi:10.1111/cgf.13801
- [16] J. B. Mander, and C.-T. Cheng, *Seismic resistance of bridge piers based on damage avoidance design*, Technical Report Technical Report NCEER-97-0014, University at Buffalo, State University of New York, 1997.
- [17] MATLAB version R2018a, The MathWorks Inc., Natick, Massachusetts, 2018.
- [18] G+D Computing 2005. *Straus7 User’s Manual*.
- [19] M. Froli, and F. Laccone, and D. Maesano, “The TVT Glass Pavilion: Theoretical Study on a Highly Transparent Building Made with Long-Spanned TVT Portals Braced with Hybrid Glass-Steel Panels,” *Buildings*, 7(2):50, 2017. doi:10.3390/buildings7020050